ORIGINAL RESEARCH

Gambogic acid-loaded magnetic Fe$_3$O$_4$ nanoparticles inhibit Panc-1 pancreatic cancer cell proliferation and migration by inactivating transcription factor ETS1

Cailian Wang[1]
Haijun Zhang[1]
Yan Chen[1]
Fangfang Shi[1]
Baoan Chen[2,3]

[1]Department of Oncology, [2]Department of Hematology, Zhongda Hospital, [3]Faculty of Oncology, Medical School, Southeast University, Nanjing, People's Republic of China

Correspondence: Baoan Chen
Department of Hematology, Zhongda Hospital, Medical School, Southeast University, Nanjing 210009, People's Republic of China
Tel +86 25 8327 2006
Fax +86 25 8327 2011
Email cba8888@hotmail.com

Background: E26 transformation-specific sequence-1 (ETS1) transcription factor plays important roles in both carcinogenesis and the progression of a wide range of malignancies. Aberrant ETS1 expression correlates with aggressive tumor behavior and a poorer prognosis in patients with various malignancies. The aim of the current study was to evaluate the efficacy of a drug delivery system utilizing gambogic acid-loaded magnetic Fe$_3$O$_4$ nanoparticles (GA-MNP-Fe$_3$O$_4$) on the suppression of ETS1-mediated cell proliferation and migration in Panc-1 pancreatic cancer cells.

Methods: The effects caused by GA-MNP-Fe$_3$O$_4$ on the proliferation of Panc-1 pancreatic cancer cells were evaluated using a MTT (3-(4,5-dimethylthiazol-2-yl)-2,5-diphenyltetrazolium bromide) assay while inhibition of tumor cell migration was investigated in a scratch assay. The expressions of ETS1, cyclin D1, urokinase-type plasminogen activator (u-PA), and VEGF (vascular endothelial growth factor) were examined by Western blot to elucidate the possible mechanisms involved.

Results: In Panc-1 pancreatic cancer cells, we observed that application of GA-MNP-Fe$_3$O$_4$ was able to suppress cancer cell proliferation and prevent cells from migrating effectively. After treatment, Panc-1 pancreatic cancer cells showed significantly decreased expression of ETS1, as well as its downstream target genes for cyclin D1, u-PA, and VEGF.

Conclusion: Our novel finding reaffirmed the significance of ETS1 in the treatment of pancreatic cancer, and application of GA-MNP-Fe$_3$O$_4$ nanoparticles targeting ETS1 should be considered as a promising contribution for better pancreatic cancer care.

Keywords: ETS1 transcription factor, gambogic acid, pancreatic cancer, magnetic nanoparticles

Introduction

Pancreatic cancer is characterized by late detection, a poor prognosis, and aggressive metastasis.[1] Median survival for patients after initial diagnosis is as short as 6 months.[2] Even in cases where the cancer is diagnosed at an early resectable stage, the 5-year survival is still only 22%.[3] Due to pancreatic cancer being one of the most malignant types of cancer to treat, a better understanding of the molecular mechanism involved in pancreatic cancer and subsequent identification of a specific molecular target are necessary to develop novel and more effective therapeutics.

E26 transformation-specific sequence-1 (ETS1) is a proto-oncoprotein belonging to the ETS protein family of transcription factors. These transcription factors contain a conserved winged helix-turn-helix DNA binding domain and regulate gene expression

by binding to so-called ETS-binding sequences found in the promoter/enhancer regions of their target genes.[4] ETS1 plays a role in the regulation of physiologic processes such as cell proliferation and differentiation, and there is much evidence suggesting important roles for ETS1 in carcinogenesis and progression of a wide range of malignancies, including pancreatic cancer.[5–9] Transcriptional silencing of ETS1 could suppress angiogenesis of pancreatic cancer efficiently.[10] Correlation between ETS1 overexpression and aggressive tumor behavior suggests that ETS1 may be an attractive molecular target for cancer therapy.

Gambogic acid (GA), the natural compound extracted from gamboges, has recently been established as a potent anticancer agent that can inhibit the growth of a wide variety of tumor cells, including hepatocellular carcinoma, pulmonary carcinoma, gastric cancer, breast cancer, and pancreatic cancer cells.[11–15] However, the mechanism by which GA exerts its anticancer effect, particularly along with its target proteins, has not been clarified. Whether the GA-induced anticancer effect is mediated by ETS1 remains to be addressed. In addition, the therapeutic effect of GA is limited due to its poor water solubility.[16] Therefore, efforts should be made to develop new drug delivery techniques to increase water solubility which could advance the biodistribution of GA, enhance its deposition in tumor sites, and improve its therapeutic efficacy.

Various types of nanosized drug carriers, such as metal nanomaterials, liposomes, polymeric micelles, and dendrimers, have been investigated in cancer therapy in order to minimize the side effects of anticancer drugs, increase the water solubility of drugs, and enhance antitumoral drug efficacy.[17,18] Among them, magnetic Fe_3O_4 nanoparticles (MNP-Fe_3O_4), a biocompatible and superparamagnetic nanomaterial with satisfactory chemical stability and low toxicity, is widely used for targeted drug carriers with target-orientation and sustained-release properties.[19–23]

The aim of this study was to gain an insight into the involvement of ETS1 transcription factor in GA-loaded MNP-Fe_3O_4-induced suppression of Panc-1 pancreatic cancer cell proliferation and migration. To the best of our knowledge, no study has been carried out using GA as an inhibitor of the ETS1 transcription factor in pancreatic cancer treatment thus far. Here, for the first time, we investigate the probability and properties of GA-loaded MNP-Fe_3O_4 in the inhibition of Panc-1 pancreatic cancer cell proliferation and migration through inactivating transcription factor ETS1. GA was loaded onto MNP-Fe_3O_4 (GA-MNP-Fe_3O_4) as a drug delivery system. We then identified the viability/proliferation effects of GA-MNP-Fe_3O_4 on Panc-1 pancreatic cancer cells and investigated inhibition of cell migration. We further measured the expression of ETS1, cyclin D1, urokinase-type plasminogen activator (u-PA), and vascular endothelial growth factor (VEGF) to study the mechanisms possibly involved.

Materials and methods
Main chemicals and apparatus
GA (Kanion Pharmaceutical Co, Ltd, Jiangsu, China) was dissolved in dimethylsulfoxide (Sigma Aldrich, St Louis, MO), stored at −20°C, and then diluted as needed in RPMI (Roswell Park Memorial Institute) 1640 medium (Gibco/BRL, Carlsbad, CA). Iron (III) chloride hexahydrate ($FeCl_3 \cdot 6H_2O$) and iron (II) chloride tetrahydrate ($FeCl_2 \cdot 4H_2O$) were obtained from Sinopharm Chemical Reagent Co, Ltd, (Shanghai, China). Ammonium hydroxide was purchased from Shanghai Lingfeng Chemical Reagent Co, Ltd, (Shanghai, China). Monoclonal antibodies, including ETS1, cyclin D1, u-PA, and VEGF, were purchased from Santa Cruz Biotechnology (Santa Cruz, CA). The horseradish peroxidase-conjugated IgG antibody was obtained from Nanjing KeyGen Biotech Inc, (Nanjing, China). 3-(4, 5-Dimethylthiazol-2-yl)-2, 5-diphenyltetrazolium bromide (MTT) was obtained from Sigma and stored in the dark. All other reagents were of analytical grade. The transmission electron microscopic images were obtained using a JEM-2100 transmission electron microscope. The microscopic images were taken using an Olympus IX51 inverted microscope. The optical density (OD) at 492 nm was recorded by a multiwell spectrophotometer reader (Thermo Labsystems, Vantta, Finland).

Synthesis of MNP-Fe_3O_4
Magnetic Fe_3O_4 nanoparticles were prepared by coprecipitation of Fe (III) and Fe (II) with ammonium hydroxide in a nitrogen environment. In a typical synthetic experiment, $FeCl_3 \cdot 6H_2O$ 2.61 g and $FeCl_2 \cdot 4H_2O$ 1.04 g were dissolved in 100 mL of deionized water and heated to 80°C, followed by slow addition of 10 mL of ammonium hydroxide with vigorous stirring for 20 minutes. The products were cooled to room temperature and extracted using a magnet. Finally, after being washed with ethanol and deionized water, the products were lyophilized and stored at room temperature.

Preparation of GA-loaded MNP-Fe_3O_4
GA-MNP-Fe_3O_4 was prepared as previously described.[15,24] In brief, MNP-Fe_3O_4 were well distributed in RPMI-1640 medium with 10% heated inactivated fetal bovine serum

using ultrasound treatment in order to obtain an MNP-Fe$_3$O$_4$ colloidal suspension. GA at different concentrations was conjugated with the above MNP-Fe$_3$O$_4$ colloidal suspension by mechanical absorption polymerization at 4°C for 48 hours to achieve the formation of GA-MNP-Fe$_3$O$_4$ which acted as a drug delivery system.

Cell culture

Panc-1 pancreatic cancer cells, obtained from the Shanghai Institute of Cell Biology, Chinese Academy of Sciences, were cultured in RPMI-1640 supplemented with 10% heat-inactivated fetal bovine serum, 100 U/mL penicillin, and 100 µg/mL streptomycin at 37.0°C in humidified air with 5% CO$_2$. The cells were in log phase prior to the following experiments.

Cell viability/proliferation assay

The antiproliferation effects of MNP-Fe$_3$O$_4$, GA, and GA-MNP-Fe$_3$O$_4$ were studied with MTT assays using Panc-1 pancreatic cancer cells. Cells at 1×10^5/mL were seeded into 96-well plates and incubated for 24 hours. The growth medium was then replaced with 200 µL of prepared medium containing either GA alone or GA-MNP-Fe$_3$O$_4$, in which the GA concentration was 0, 0.25, 0.5, 1, and 2 µmol/L. The cells were also treated by MNP-Fe$_3$O$_4$ alone for evaluation of its cytotoxicity. Cells without any treatment were used as the control group. The cells were further incubated for 48 hours, and their relative viability was assessed using MTT assays. In brief, MTT solutions were added after the treatments and incubated for a further 4 hours. Dimethylsulfoxide was added to solubilize the formazan crystal, and an optical density of 492 was recorded. The cell viability fraction (%) was calculated as follows:

$$\text{OD}_{492 \text{ nm in test cells}}/\text{OD}_{492 \text{ nm in control cells}} \times 100\%$$

Scratch assay

A cell migration assay was carried out by scratch assay. Initially, cells were plated in 6-well plates and allowed to form a confluent monolayer. Then the cell-surface was scratched using pipette tips and washed with phosphate buffer solution. After that, the cells were treated according to the above methods, allowed to fill the scratched area, and monitored over the course of 48 hours. Images were taken using an Olympus IX51 inverted microscope. Cell motility was quantified by measuring the distance between the migrating cell boundaries.

Western blot analysis

After the different treatments, the expressions of ETS1, cyclin D1, u-PA, and VEGF were detected by Western blot. Briefly, total protein was isolated and subjected to sodium dodecyl sulfate polyacrylamide gel electrophoresis, and transferred to a polyvinylidene fluoride membrane. After being blocked, the membrane was incubated with primary monoclonal antibodies for either anti-ETS1, cyclin D1, u-PA, VEGF, or anti-β-actin overnight at 4°C, and subsequently incubated with horseradish peroxidase-conjugated IgG antibody as the secondary antibody for one hour at room temperature. The protein bands were detected using an enhanced chemiluminescence detection system (Amersham, UK). After normalization by the corresponding expression of β-actin, protein expression of ETS1, cyclin D1, u-PA, and VEGF was determined by densitometry scans.

Statistical analysis

All the data are presented as the mean ± standard deviation. The F-test was used for significance testing, and $P < 0.05$ was considered to be statistically significant. All tests were performed using the Statistical Package for Social Science (version 13.0; SPSS Inc, Chicago, IL).

Results and discussion
Characterization of MNP-Fe$_3$O$_4$

A representative transmission electron microscopic image of the synthesized MNP-Fe$_3$O$_4$ is shown in Figure 1. From the transmission electron microscopic image, the nanoparticles had a spherical shape with a diameter of about 20 nm. The particles had suitable dimensions to escape rapid renal excretion, as well as to avoid components of the reticular endothelial system, thus facilitating potentially passive targeting
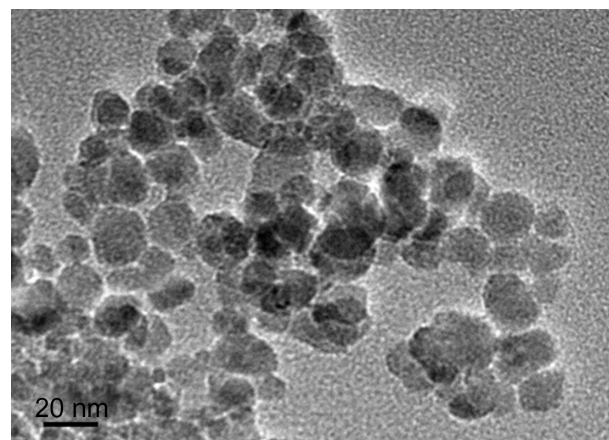

Figure 1 Transmission electron microscope image of magnetic Fe$_3$O$_4$ nanoparticles.

of drugs to tumor tissue via the enhanced permeation and retention effect and active targeting with target orientation of the magnetic field, thereby increasing drug accumulation in tumor cells after endocytosis.[25]

Drug carrier role of MNP-Fe₃O₄

GA ($C_{38}H_{44}O_8$) has five prenyl groups and six asymmetric centers (Figure 2A) and is a potent anticancer agent, but is limited in clinical administration due to its poor water solubility.[16] Therefore, we sought to identify the potential benefit of a drug delivery system containing GA-MNP-Fe₃O₄ for cancer therapy in the present study. Figure 2B illustrates the preparation process for the drug delivery system. As shown in Figure 2C, unlike GA solution, no precipitation of GA was noted in the colloidal suspension of the GA-MNP-Fe₃O₄ drug delivery system after 2 months of storage at 4°C, indicating that the solubility of GA was improved and the drug delivery system was stable during storage.

Antiproliferative effect in vitro

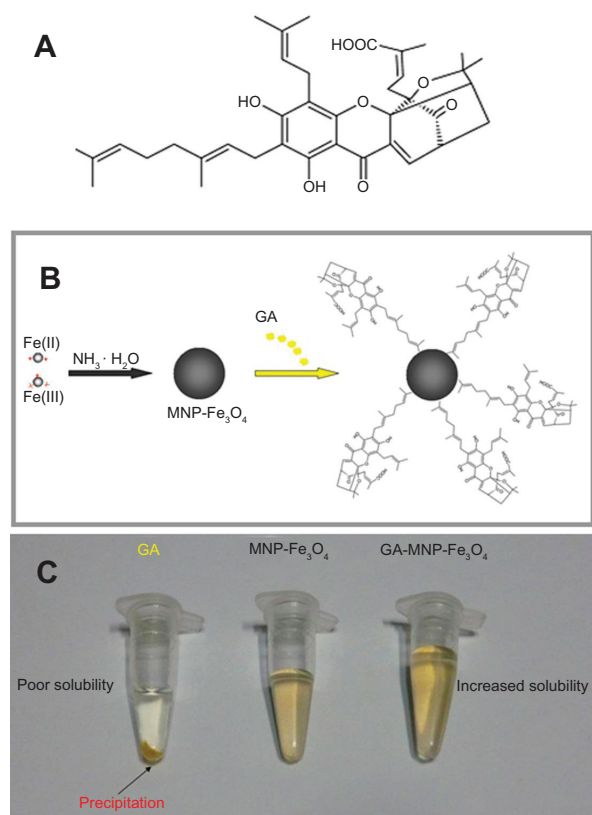Inhibition of cell viability/proliferation is one of major mechanisms by which chemotherapeutic agents kill cancer cells.[26]

The results of cell viability after different treatments are shown in Figure 3. Cytotoxicity testing of a nanomaterial is the first-level evaluation before its biomedical application. When treated with MNP-Fe₃O₄ 20 µg/mL, about 95% of the cells survived (Figure 3, blue column), which is consistent with our previous report.[15] The results suggest that the MNP-Fe₃O₄ synthesized in this study lacked cytotoxicity, thus ensuring a wide potential range of applications in the field of biomedical science and cancer therapy. GA as a single agent could inhibit the viability/proliferation of cancer cells (Figure 3, yellow column). Compared with GA alone, the viability of Panc-1 cells treated by GA-MNP-Fe₃O₄ obviously decreased (Figure 3, red column). Hence GA-MNP-Fe₃O₄ suppressed cancer cell proliferation effectively. Meanwhile, our results also indicate that the antiproliferative effect increased with increasing concentrations of GA, suggesting a dose-dependent effect in vitro. The increased antiproliferative effect may be due to improved GA cellular uptake by the GA-MNP-Fe₃O₄ drug delivery system, which increases the water solubility of GA through the endocytosis pathway and then induces release of GA from the MNP-Fe₃O₄ in cancer cells to promote efficient cell killing, which is a common characteristic of nanoparticle-based drug delivery systems.[27,28]

The IC$_{50}$ value, ie, the concentration of a drug that inhibits cell growth by 50% in different treatments of GA and GA-MNP-Fe₃O₄, was determined from the above dose responses. As shown in Figure 4, the IC$_{50}$ value of free GA for the cancer cells was 1.29 µmol/L, and GA-MNP-Fe₃O₄ could alter the IC$_{50}$ value to 0.52 µmol/L. The lower IC$_{50}$ of GA-MNP-Fe₃O₄ for the drug delivery system could improve the therapeutic efficacy without high usage of GA to inhibit cancer cell proliferation.

Inhibition of cell migration

Migration and invasion of cancer cells are key steps of tumor metastasis.[29] The effect of GA-MNP-Fe₃O₄ on the motility
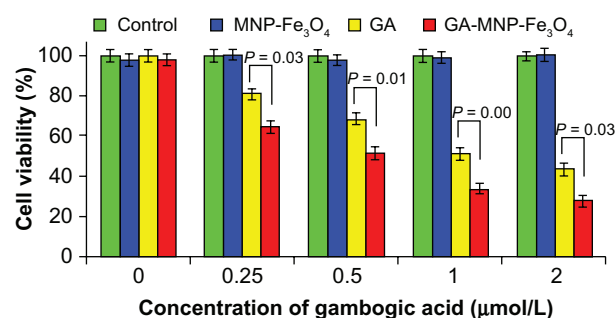

Figure 2 Chemical structure of GA (**A**), schematic representation (**B**), and photographic image (**C**) of the GA-loaded MNP-Fe₃O₄ drug delivery system.
Abbreviations: GA, gambogic acid; MNP-Fe₃O₄, magnetic Fe₃O₄ nanoparticles.

Figure 3 Antiproliferative effect of GA and GA-MNP-Fe₃O₄ on Panc-1 pancreatic cancer cells.
Note: Data are expressed as the mean ± standard deviation (n = 3).
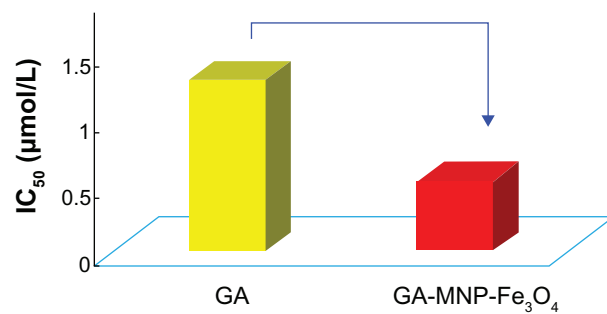**Abbreviations:** GA, gambogic acid; MNP-Fe₃O₄, magnetic Fe₃O₄ nanoparticles.

Figure 4 IC_{50} of GA and GA-MNP-Fe_3O_4 for Panc-1 pancreatic cancer cells.
Abbreviations: GA, gambogic acid; MNP-Fe_3O_4, magnetic Fe_3O_4 nanoparticles.

of Panc-1 pancreatic cancer cells was measured in a scratch assay. GA alone resulted in a decrease in cell motility (Figure 5C), while no effects were observed on the motility of MNP-Fe_3O_4 (Figure 5B). However, compared with GA alone, GA-MNP-Fe_3O_4 (Figure 5D) dramatically inhibited Panc-1 pancreatic cancer cell migration. Cell motility was also quantified by measuring the distance between the migrating cell boundaries (Figure 5E). These results suggest that GA-MNP-Fe_3O_4 is highly effective in preventing Panc-1 cell migration.

Potential mechanisms of inhibition of tumor cell proliferation and migration

ETS1 is induced by and is required for the activation of several genes involved in proliferation, remodeling of the
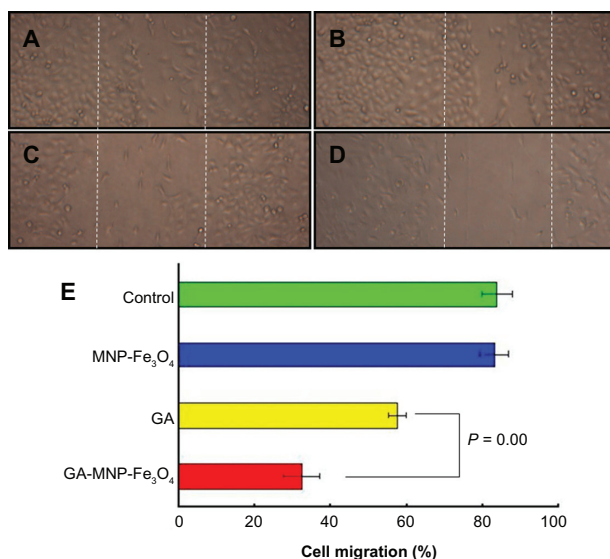
extracellular matrix, and angiogenesis, such as u-PA and VEGF, all of which carry ETS-responsive elements in their promoters.[30] Aberrant ETS1 expression appears to be associated with the pathophysiology of some malignancies,[5–9] so it has been suggested that pharmacological inhibition of ETS1 transcriptional activity may prove useful as a novel anticancer strategy. Recent reports have suggested transcriptional silencing of ETS1 could efficiently suppress angiogenesis in pancreatic cancer.[10] The results from our in vitro studies have demonstrated that GA-MNP-Fe_3O_4 resulted in synergistic inhibition of cell proliferation and migration in pancreatic cancer. To address the question whether GA-MNP-Fe_3O_4 inhibited cell proliferation and migration through inactivating transcription factor ETS1, the expression of ETS1 and its downstream target genes in Panc-1 pancreatic cancer cells exposed to the different treatments were examined by Western blot. We focused on cyclin D1, u-PA, and VEGF, which mediate proliferation, migration, and angiogenesis in several cancers and have been reported to be direct targets of ETS transcription factors.[4] As shown in Figure 6, when the Panc-1 pancreatic cancer cells were treated with GA alone and with GA-MNP-Fe_3O_4 for 48 hours, not only the

Figure 5 Inhibition of Panc-1 pancreatic cancer cell migration after the different treatments for 48 hours. (**A**) Untreated cells as controls, (**B**) MNP-Fe_3O_4, (**C**) GA alone, (**D**) GA-MNP-Fe_3O_4, and (**E**) quantified cell motility.
Notes: Concentrations of GA and MNP-Fe_3O_4 are 1 µmol/L and 20 µg/mL, respectively.
Abbreviations: GA, gambogic acid; MNP-Fe_3O_4, magnetic Fe_3O_4 nanoparticles.
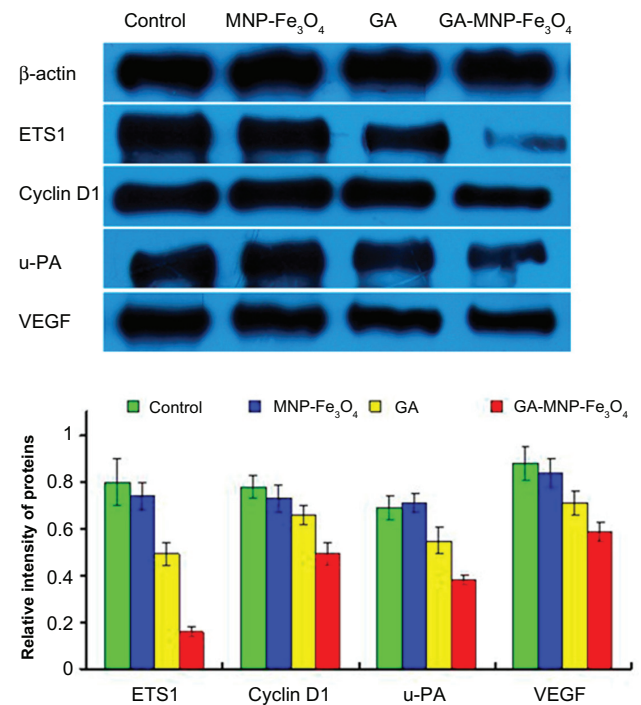

Figure 6 Expression of ETS1, cyclin D1, u-PA, and VEGF protein in Panc-1 pancreatic cancer cells by Western blot after treatment with GA and/or MNP-Fe_3O_4 for 48 hours.
Notes: Concentrations of GA and MNP-Fe_3O_4 are 1 µmol/L and 20 µg/mL, respectively.
Abbreviations: GA, gambogic acid; MNP-Fe_3O_4, magnetic Fe_3O_4 nanoparticles; ETS1, E26 transformation-specific sequence-1 transcriptional factor; u-PA, urokinase-type plasminogen activator; VEGF, vascular endothelial growth factor.
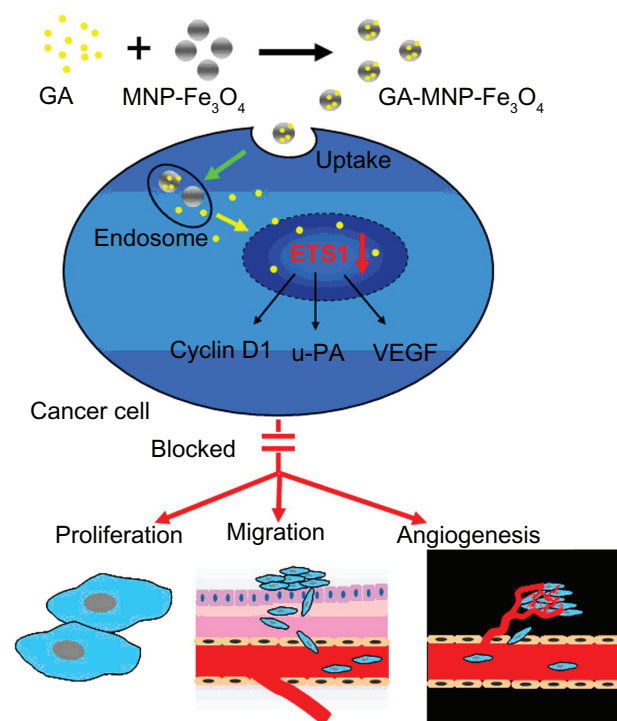
Figure 7 Schematic illustration of regulation based on ETS1 by GA-MNP-Fe$_3$O$_4$.
Abbreviations: ETS1, E26 transformation-specific sequence-1 transcriptional factor; GA, gambogic acid; MNP-Fe$_3$O$_4$, magnetic Fe$_3$O$_4$ nanoparticles; u-PA, urokinase-type plasminogen activator; VEGF, vascular endothelial growth factor.

level of ETS1 but also that of cyclin D1, u-PA, and VEGF protein was significantly downregulated compared with the control group. It should be noted that downregulated levels in the GA-MNP-Fe$_3$O$_4$ group were lower than those in the GA group ($P < 0.05$). However, they were not obviously altered when the cells were treated with MNP-Fe$_3$O$_4$ alone ($P > 0.05$). Cyclin D is the first cyclin expressed in the cell cycle after stimulation by mitogenic signals, and stimulates cells to enter the cell cycle and complete the G1/S phase transition.[31] The suppressive effect of GA-MNP-Fe$_3$O$_4$ on expression of the cell cycle-related gene, cyclin D1, revealed that GA-MNP-Fe$_3$O$_4$ might inhibit Panc-1 pancreatic cancer cell proliferation mainly through cell cycle arrest. Overexpression of u-PA triggers a series of proteolytic and signaling events that promote invasion and metastasis in various cancers.[32] Moreover, we found that GA-MNP-Fe$_3$O$_4$ inhibited migration behavior through suppression of u-PA in Panc-1 pancreatic cancer cells. Angiogenesis plays a critical role in tumor progression. VEGF is an important proangiogenic molecule, which plays a crucial role in tumor angiogenesis. Inhibition of VEGF activity often results in inhibition of tumor growth or even tumor regression.[33] Furthermore, we showed that GA-MNP-Fe$_3$O$_4$ significantly downregulated expression of VEGF, suggesting that it may

be a viable strategy in antiangiogenesis and anticancer therapies for pancreatic cancer. These data indicate that the effects could be in part attributed to downregulation of transcription factor ETS1. GA-MNP-Fe$_3$O$_4$ inhibits Panc-1 pancreatic cancer cell proliferation and migration by targeting cyclin D1, u-PA, and VEGF via inactivation of ETS1.

Based on the above studies, Figure 7 schematically illustrates the possible processes by which the GA-MNP-Fe$_3$O$_4$ drug delivery system inhibits cancer cell proliferation and migration. Firstly, GA was conjugated with MNP-Fe$_3$O$_4$ to construct GA-MNP-Fe$_3$O$_4$, which acted as a drug delivery system. This drug delivery system increased the water solubility of GA. After endocytosis, the Panc-1 pancreatic cancer cells showed significantly decreased expression of ETS1, as well as its downstream target genes, cyclin D1, u-PA, and VEGF protein, to suppress cancer cell proliferation and prevent cells from migrating effectively.

Conclusion

GA-MNP-Fe$_3$O$_4$ could inhibit proliferation and migration of Panc-1 pancreatic cancer cells. This study further demonstrates that the effects could be in part attributable to downregulation of transcription factor ETS1. Thus, its downstream target genes which mediate cell proliferation, migration, and angiogenesis, ie, cyclin D1, u-PA, and VEGF, were downregulated as well. All these characteristics suggest that GA-MNP-Fe$_3$O$_4$ is a promising strategy targeting ETS1 for the treatment of pancreatic cancer.

Acknowledgments

Disclosure

The authors report no conflicts of interest in this work.

References

1. Khanna A, Mahalingam K, Chakrabarti D, Periyasamy G. ETS-1 expression and gemcitabine chemoresistance in pancreatic cancer cells. *Cell Mol Biol Lett*. 2011;16:101–113.
2. Tempero MA, Berlin J, Ducreux M, et al. Pancreatic cancer treatment and research: an international expert panel discussion. *Ann Oncol*. 2011;22:1500–1506.
3. Jemal A, Siegel R, Xu J, Ward E. Cancer Statistics, 2010. *CA Cancer J Clin*. 2010;60:277–300.
4. Oikawa T, Yamada T. Molecular biology of the ETS family of transcription factors. *Gene*. 2003;303:11–34.
5. Fujimoto J, Aoki I, Toyoki H, et al. Clinical implications of expression of ETS-1 related to angiogenesis in metastatic lesions of ovarian cancers. *Oncology*. 2004;66:420–428.

6. Ozaki I, Mizuta T, Zhao G, et al. Induction of multiple matrix metalloproteinase genes in human hepatocellular carcinoma by hepatocyte growth factor via a transcription factor ETS-1. *Hepatol Res*. 2003;27:289–301.

7. Yamaguchi E, Nakayama T, Nanashima A, et al. ETS-1 proto-oncogene as a potential predictor for poor prognosis of lung adenocarcinoma. *Tohoku J Exp Med*. 2007;213:41–50.

8. Ito H, Duxbury M, Benoit E, et al. Prostaglandin E2 enhances pancreatic cancer invasiveness through an ETS-1-dependent induction of matrix metalloproteinase-2. *Cancer Res*. 2004;64:7439–7446.

9. Li YY, Wu Y, Tsuneyama K, Baba T, Mukaida N. Essential contribution of ETS-1 to constitutive Pim-3 expression in human pancreatic cancer cells. *Cancer Sci*. 2009;100:396–404.

10. Lefter LP, Dima S, Sunamura M, et al. Transcriptional silencing of ETS-1 efficiently suppresses angiogenesis of pancreatic cancer. *Cancer Gene Ther*. 2009;16:137–148.

11. Guo QL, You QD, Wu ZQ, Yuan ST, Zhao L. General gambogic acids inhibited growth of human hepatoma SMMC-7721 cells in vitro and in nude mice. *Acta Pharmacol Sin*. 2004;25:769–774.

12. Yu J, Guo QL, You QD, et al. Gambogic acid-induced G(2)/M phase cell-cycle arrest via disturbing CDK7-mediated phosphorylation of CDC2/p34 in human gastric carcinoma BGC-823 cells. *Carcinogenesis*. 2007;28:632–638.

13. Kasibhatla S, Jessen KA, Maliartchouk S, et al. A role for transferrin receptor in triggering apoptosis when targeted with gambogic acid. *Proc Natl Acad Sci U S A*. 2005;102:12095–12100.

14. Wu ZQ, Guo QL, You QD, Zhao L, Gu HY. Gambogic acid inhibits proliferation of human lung carcinoma SPC-A1 cells in vivo and in vitro and represses telomerase activity and telomerase reverse transcriptase mRNA expression in the cells. *Biol Pharm Bull*. 2004;27:1769–1774.

15. Wang C, Zhang H, Chen B, Yin H, Wang W. Study of the enhanced anticancer efficacy of gambogic acid on Capan-1 pancreatic cancer cells when mediated via magnetic Fe$_3$O$_4$ nanoparticles. *Int J Nanomedicine*. 2011;6:1929–1935.

16. Zhu X, Zhang C, Wu XL, et al. Preparation, physical properties, and stability of gambogic acid-loaded micelles based on chitosan derivatives. *Drug Dev Ind Pharm*. 2008;34:2–9.

17. Wang JQ, Sui MH, Fan WM. Nanoparticles for tumor targeted therapies and their pharmacokinetics. *Curr Drug Metab*. 2010;11:129–141.

18. Zhang HJ, Chen BA, Jiang H, Wang CL, Wang HP, Wang XM. A strategy for ZnO nanorod mediated multi-mode cancer treatment. *Biomaterials*. 2011;32:1906–1914.

19. Wu WW, Chen BA, Cheng J, et al. Biocompatibility of Fe$_3$O$_4$/DNR magnetic nanoparticles in the treatment of hematologic malignancies. *Int J Nanomedicine*. 2010;5:1079–1084.

20. Wang J, Chen BA, Cheng J, et al. Apoptotic mechanism of human leukemia K562/A02 cells induced by magnetic iron oxide nanoparticles co-loaded with daunorubicin and 5-bromotetrandrin. *Int J Nanomedicine*. 2011;6:1027–1034.

21. Lin BL, Shen XD, Cui S. Application of nanosized Fe$_3$O$_4$ in anticancer drug carriers with target-orientation and sustained-release properties. *Biomed Mater*. 2007;2:132–134.

22. Zhu A, Yuan L, Jin W, et al. Polysaccharide surface modified Fe$_3$O$_4$ nanoparticles for camptothecin loading and release. *Acta Biomater*. 2009;5:1489–1498.

23. Chin SF, Iyer KS, Saunders M, et al. Encapsulation and sustained release of curcumin using superparamagnetic silica reservoirs. *Chem Eur J*. 2009;15:5661–5665.

24. Chen BA, Liang YQ, Wu WW, et al. Synergistic effect of magnetic nanoparticles of Fe$_3$O$_4$ with gambogic acid on apoptosis of K562 leukemia cells. *Int J Nanomedicine*. 2009;4:251–259.

25. Zhang DW, Zhang H, Nie J, Yang J. Synthesis and self-assembly behavior of pH-responsive amphiphilic copolymers containing ketal functional groups. *Polym Int*. 2010;59:967–974.

26. Huang H, Chen D, Li S, et al. Gambogic acid enhances proteasome inhibitor-induced anticancer activity. *Cancer Lett*. 2011;301:221–228.

27. Bareford LA, Swaan PW. Endocytic mechanisms for targeted drug delivery. *Adv Drug Deliv Rev*. 2007;59:748–758.

28. Yoo HS, Lee KH, Oh JE, Park TG. In vitro and in vivo anticancer activities of nanoparticles based on doxorubicin-PLGA conjugates. *J Control Release*. 2000;68:419–431.

29. Wang L, Kuang L, Pan X, et al. Isoalvaxanthone inhibits colon cancer cell proliferation, migration and invasion through inactivating Rac1 and AP-1. *Int J Cancer*. 2010;127:1220–1229.

30. Taniguchi H, Fujiwara Y, Doki Y, et al. Gene therapy using eTS-1 transcription factor decoy for peritoneal dissemination of gastric cancer. *Int J Cancer*. 2007;121:1609–1617.

31. Peng Y, Li H, Wu M, et al. NGX6 inhibits AP-1 and ETS-1 expression and down-regulates cyclin D1 in human colorectal cancer. *Acta Biochim Biophys Sin (Shanghai)*. 2009;41:504–514.

32. Gupta R, Chetty C, Bhoopathi P, et al. Downregulation of uPA/uPAR inhibits intermittent hypoxia-induced epithelial-mesenchymal transition (EMT) in DAOY and D283 medulloblastoma cells. *Int J Oncol*. 2011;38:733–744.

33. Lu N, Yang Y, You QD, et al. Gambogic acid inhibits angiogenesis through suppressing vascular endothelial growth factor-induced tyrosine phosphorylation of KDR/Flk-1. *Cancer Lett*. 2007;258:80–89.